THE BALTIC JOURNAL
OF ROAD AND BRIDGE ENGINEERING
2026/21(1)

ISSN 1822-427X/eISSN 1822-4288
2026 Volume 21 Issue 1: 125–150
https://doi.org/10.7250/bjrbe.2026-21.675

INFLUENCE OF INTERFACE BONDING CONDITION AND BASE LAYER ELASTIC MODULUS ON ASPHALT PAVEMENT STRUCTURE MECHANICAL RESPONSE TO NON-UNIFORM LOADS

LANA ELABBAS ABDELHALIEM BABIKER[1–3], XIN JIANG[1–3,*], CANYANG CUI[1–3], YANGCHEN LU[1–3], MIAN ZHANG[1–3], YANG XUE[1–3], YANJUN QIU[1–3]

[1]*School of Civil Engineering, Southwest Jiaotong University, Chengdu 610031, China*

[2]*Highway Engineering Key Laboratory of Sichuan Province, Southwest Jiaotong University, Chengdu 610031, China*

[3]*MOE Key Laboratory of High-speed Railway Engineering, Southwest Jiaotong University, Chengdu 610031, China*

Received 25 March 2025; accepted 18 February 2026

Abstract. This study established the ratio of the base layer's elastic modulus to that of the surface layer R_m as a key variable to systematically investigate how the base layer's elastic modulus influences the mechanical response and service life of flexible pavement. A

* Corresponding author. E-mail: xjiang01@163.com

Lana Elabbas Abdelhaliem BABIKER (ORCID ID 0009-0009-3049-739X)
Xin JIANG (ORCID ID 0000-0002-3044-5495)
Canyang CUI (ORCID ID 0000-0002-3959-5473)
Yangchen LU (ORCID ID 0009-0004-2758-0946)
Mian ZHANG (ORCID ID 0000-0002-3235-9398)
Yang XUE (ORCID ID 0009-0008-9681-0484)
Yanjun QIU (ORCID ID 0000-0002-2250-5363)

three-dimensional finite element model of a three-layer pavement system was analysed, using EverStressFE, with a constant surface layer modulus and a variable base layer modulus. The analysis included two important interfacial bonding conditions: full bonding and full slip. It also considered that the actual wheel loads are not uniform but rather follow concave and convex distribution patterns. The mechanical responses, including deflection at the top of the asphalt layer, tensile strain at the bottom of the asphalt layer ε_{xx}, and vertical compressive strain at the top of the subgrade ε_{zz}, were quantified to predict fatigue life (for cracking) and rutting life (for permanent deformation). The results indicated that the maximum deflection reached 0.53 mm under a full slip condition with a convex load distribution at R_m = 0.75. Critical tensile strains at the bottom of the asphalt layer were most severe under full slip with a convex load, reaching 348 × 10^{-6}, while the fully bonded, concave case resulted in a much lower value of 83 × 10^{-6}. Similarly, the maximum vertical compressive strain on the subgrade was 365 × 10^{-6} for the fully slipped, convex case compared to 250 × 10^{-6} for the fully bonded, concave case. A lower R_m value under full slip with a concave load distribution significantly reduced the pavement lifespan, with predicted fatigue life decreasing by over 60% and rutting life by nearly 45% compared to the fully bonded case. On the other hand, a convex load distribution greatly increased the pavement's bearing capacity by raising the critical strain thresholds and lengthening the expected service life. These findings underscore the paramount importance of interface bonding and load distribution patterns, suggesting that they can outweigh the influence of the base layer's modulus alone on pavement design.

Keywords: bonding condition, elastic modulus, finite element method, mechanical response, non-uniform wheel load.

Introduction

Understanding the various load distributions is essential for accurately predicting pavement performance (Abed et al., 2019). The mechanical responses of asphalt layers to differing load pressures can significantly influence their durability and longevity (Qian et al., 2021). For example, layers subjected to high localized stresses may demonstrate reduced lifespans due to accelerated wear and tear, while layers experiencing more uniform pressure might undergo gradual degradation over time (Dhasmana, 2020). The distribution of non-uniform loads on asphalt pavement can be categorised into two primary types: convex and concave distributions. Each type represents a distinct loading scenario that can impact the performance and longevity of the pavement (Zhu & Shi, 2021). A convex load distribution is characterised by high tire pressure concentrated over a small area of the pavement. This situation often occurs when heavy vehicles, such as trucks or buses, apply substantial force through their tires onto the road surface (Wang, 2011). The localized stress resulting from this concentrated pressure can lead to significant deformation and potential damage to the pavement structure (Singh & Sahoo, 2021), specifically, the high stress concentration can cause issues such as rutting, cracking, and other forms of distress that compromise the pavement's

integrity (Canestrari & Ingrassia, 2020). In contrast, a concave load distribution is defined by lower tire pressure that is spread over a larger area (Yao et al., 2021). This type of distribution typically occurs with lighter vehicles or under conditions where tire pressures are not optimally maintained (Szczucka-Lasota et al., 2021). While a concave distribution may lead to a more uniform stress distribution across the pavement, it does not eliminate the risks associated with load application (Poon, 2020; Wei et al., 2021). Even though the stress is distributed over a broader area, the overall lower pressure can still result in issues such as fatigue cracking over time, particularly if the pavement experiences repeated loading cycles (Norouzi et al., 2016). Furthermore, a uniform load distributes stress evenly across the pavement, concealing localized weaknesses or defects. This uniformity can delay the early detection of issues like material degradation, subgrade irregularities, or construction flaws, as the stress distribution does not cause immediate visible distress. Therefore, engineers must proactively monitor the pavement for subtle signs of failure that may only surface over time, since the uniform load does not reveal these underlying problems in the short term (Gu et al., 2019).

The elastic modulus is one of the crucial properties for understanding the behaviour of pavement layers under non-uniform loads, as it quantifies material stiffness and deformation under stress (Assogba et al., 2020; Leon & Charles, 2015). A strong elastic modulus in the surface layer is vital for protection against deformation caused by vehicle loads, minimising permanent damage and ensuring safety and functionality (Pratomo et al., 2021)). The selection of the base layer's elastic modulus varies with material types, allowing for customization to meet specific loading conditions (Leon et al., 2019; Nouri et al., 2021). Materials with a higher modulus are suitable for heavy traffic, while those with a lower modulus can be utilised for lighter loads, offering cost-effectiveness (Fan & Njuguna, 2016). Understanding how convex and concave load distributions influence stresses facilitates effective responses to prevent damage (Lorenz et al., 2022). The consideration of elastic modulus in both layers enhances pavement resilience, extending lifespan and reducing maintenance costs (Leon & Ray, 2021). This knowledge is essential for optimising performance and ensuring sustainable road infrastructure (Ijari & Paternina-Arboleda, 2024). The literature review concerning the effect of modifying the elastic modulus of the base layer provides valuable insights into how variations in material stiffness influence load distribution in pavement systems (Selsal et al., 2022). It has been noted that an increase in the elastic modulus of the base layer leads to a more favourable load distribution, thereby diminishing stress concentrations that could cause pavement distress (Jiang et al., 2024). However, numerous studies reveal significant shortcomings, such as a lack of comprehensive modelling that incorporates actual traffic conditions and load variations (Harri et al., 2009). Moreover, the effect of load distribution shape, whether circular or rectangular, is insufficiently addressed, as this does not

accurately represent real-world scenarios (Chen, 2017). The impact of the elastic modulus and its subsequent effects on load distribution are often overlooked (Oliver & Pharr, 2004). Additionally, many studies fail to consider the interactions between the base layer and other pavement layers, which may lead to incomplete conclusions regarding overall pavement performance (Bhandari et al., 2023; Haider et al., 2007; Titus-Glover et al., 2019; Zaumanis et al., 2014). This gap in knowledge emphasises the need for more integrated research that accounts for multiple variables affecting elastic modulus and load distribution to develop more effective pavement design practices.

This study directly builds upon previous FEA models by addressing their core limitations. First, to move beyond simplified load shapes, we explicitly model two specific, realistic non-uniform load distributions (convex and concave) that represent actual tire-pavement contact pressures, thereby providing a more accurate representation of real-world loading scenarios. Second, we directly investigate the often-overlooked impact of the base layer's elastic modulus, systematically varying it from 750 MPa to 9000 MPa, on critical pavement responses under these complex loads, a key factor previously identified as being neglected in the literature. Third, our analysis using EverStressFE incorporates two extreme bonding conditions (full bonding and full slip) at the layer interfaces to fully account for layer interactions, thereby addressing a critical gap identified in the literature. Through this comprehensive approach, which integrates realistic load shapes, a wide range of base layer stiffness, and interface bonding conditions, the research aims to provide new insights and predictive transfer functions that expand our knowledge of asphalt pavement performance under complex loading scenarios, ultimately offering a more integrated perspective for pavement design.

1. An overview of the elastic modulus distribution of the base layer for various materials

In practical engineering contexts, the base layer of the asphalt pavement structure can be constructed from a variety of materials, each exhibiting different stiffness levels. The typical materials include granular substances, chemically stabilised options, cement concrete, and recycled materials such as reclaimed asphalt pavement (RAP), recycled construction and demolition waste, and reclaimed concrete aggregate, among others. Numerous experimental studies conducted by researchers in recent years have demonstrated that all the aforementioned materials exhibit varying mechanical properties within the pavement structure, particularly the modulus, which is commonly used to represent material stiffness (Arshad, 2018; Arulrajah et al., 2015; Bassim & Issa, 2020; Bestgen et al., 2016;

Bilodeau & Doré, 2012; Cetin et al., 2010; da Conceição Leite et al., 2011; Ji et al., 2019; Jiang & Fan, 2013; Li et al., 2019; Miao et al., 2016; Mohammad et al., 2000; Romeo et al., 2019; Solanki et al., 2009; Yao et al., 2021). Consequently, the distribution range of modulus for four typical materials utilised in constructing the base layer is summarised as illustrated in Figure 1. This clearly indicates that the modulus variation for these materials is quite extensive, ranging from 30 MPa (granular materials) to 31 000 MPa (cement concrete). As depicted in Figure 1, cement concrete has the highest modulus, followed by chemically stabilised materials and granular materials, while recycled materials exhibit the lowest modulus due to potential damage incurred prior to recycling, such as cracks and permanent deformation. Moreover, even within the same material type, significant differences in modulus may exist, influenced by several factors including gradation, moisture content, additive proportions, and loading repetitions. For example, the minimum modulus for chemically stabilised materials is 150 MPa, while the maximum can reach 12 000 MPa according to available experimental data. In summary, the base layer material presents a broad modulus range, which will inevitably impact the performance of the asphalt layer. Therefore, this study again emphasises the importance of the modulus of the base layer on the mechanical behaviour, particularly strain distribution, of the asphalt layer. In other words, careful consideration must be given to the matching of modulus between the base layer and the asphalt layer. To comprehensively cover all representative base layer materials, a researched modulus range of 750 to 9000 MPa has been adopted for the subsequent analysis presented in this paper.

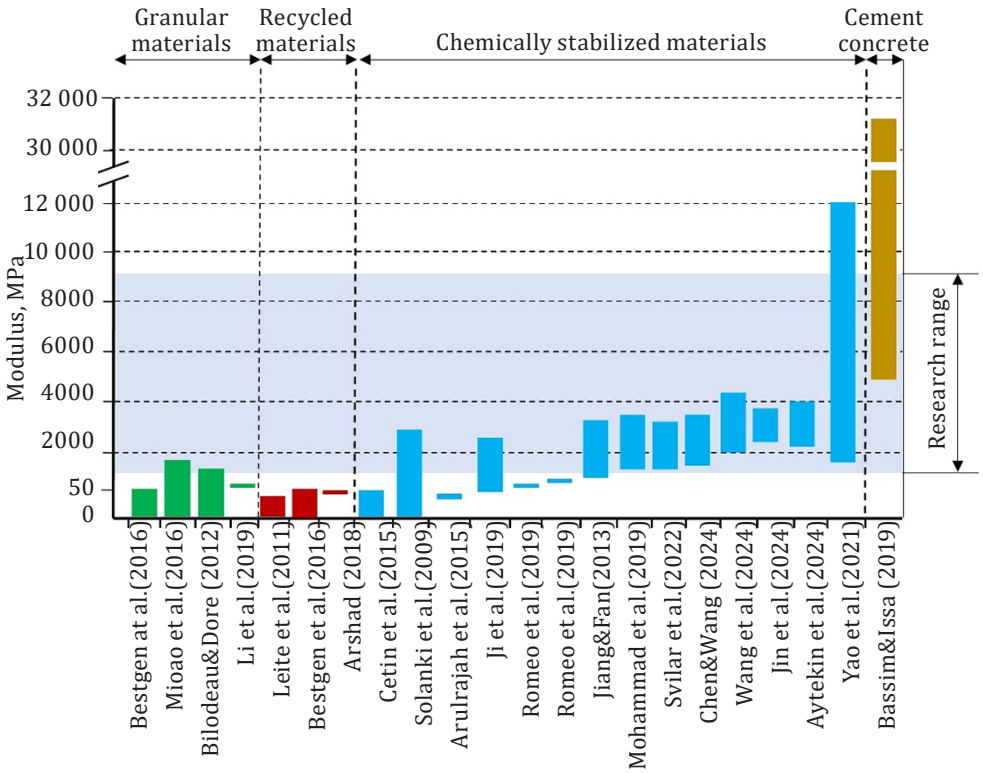

Figure 1. The modulus range of various base layer materials

3. Establishment of a three-dimensional finite element model

3.1. Tire contact pressure distribution

According to numerous studies, tire contact pressure is affected by a variety of complex factors, including tread design, tire inflation pressure, and applied load (Anghelache & Moisescu, 2012; El-Kholy & Galal, 2012; Hernandez & Al-Qadi, 2016b, 2016a, 2017; Hu & Sun, 2005, 2006; Ilse, 2015; Leon & Gay, 2020; Wang, 2005; Wang et al., 2012). The non-uniform distribution of wheel load typically produces a rectangular tire contact area. Whether the tire pattern is longitudinal or transverse, lowering tire pressure under high load conditions tends to result in a convex distribution of tire contact pressure. Conversely, increasing tire pressure under low load conditions usually leads to a concave distribution across the tread

width (Jiang et al., 2021), as shown in Figures 3a and 3b. The tire contact pressure is uniformly distributed in the central portion of the contact area, while it follows a parabolic or half-sinusoidal pattern along the edges. Calculations were performed for a single-axis dual-wheel load (25 kN per wheel), with a dual-wheel spacing of 350 mm and a tire width of 225 mm featuring a directional tread pattern. Considering the actual distribution of tire contact pressure across the tire width and in the driving direction, the wheel load was modelled to follow two types of non-uniform distribution patterns: convex and concave, as outlined in Table 1. It should be noted that, due to the directional tread pattern of the tire, the two non-uniform distribution types listed in Table 1 were designed to reflect the reduced contact area across the tire width, as demonstrated in Figure 2, with a haversine distribution assumed in the driving direction (Sofwan et al., 2019).

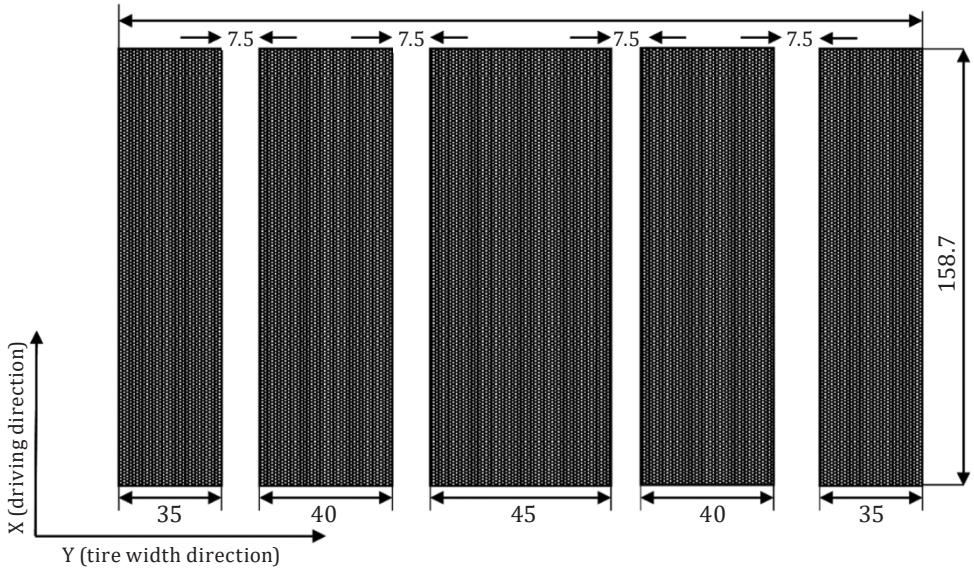

Figure 2. Simplified depiction of tire impressions (unit: mm).

Table 1. Wheel load distribution forms

Wheel load distribution	Single wheel load, kN	Wheel load force, MPa maximum value minimum value	Wheel load distribution characteristics		Note
			Along the tire width	Along the driving direction	
Convex non-uniform distribution	25	1.2	Convex	half-sinusoidal distribution	The reduction of the action area is taken into consideration, as shown in Figure 2, where X and Y indicate the driving direction and the tire width direction, respectively.
Concave non-uniform distribution	25	0.6	Concave	half-sinusoidal distribution	

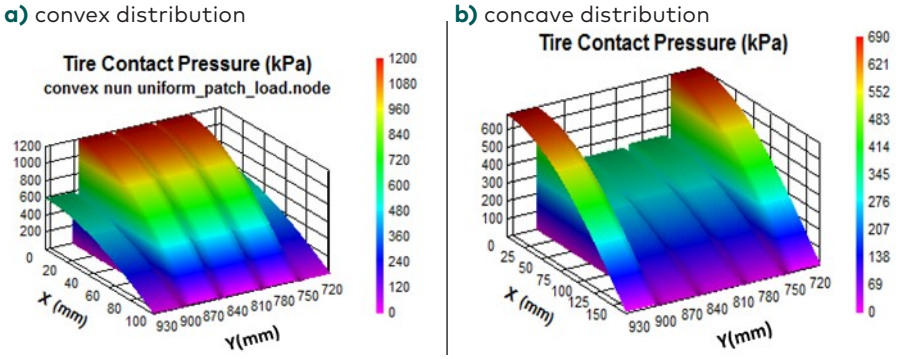

Figure 3. The non-uniform distribution of tire pressures

3.2. Description of bonding conditions

The EverStressFE software was utilised to model the bonding conditions of the asphalt pavement structure by incorporating specially processed 16-node elements at the interfaces between layers and incorporating the interface stiffness *IS*, N/mm^3. The mechanical parameter *IS* was not equivalent to the friction coefficient used in the conventional Coulomb model; rather, it was defined as the ratio of the shear stress τ, N/mm^2, at the top and bottom of the interface element to the relative shear displacement δ between nodes in the X or Y direction, as expressed in Equation (1).

$$IS = \frac{\text{Interlayer shear stress } \tau}{\text{Relative shear displacement of interlayer nodes } \delta}. \quad (1)$$

As shown in Equation (1), the bonding condition improves with an increase in interface stiffness (*IS*), indicating a trend toward a fully continuous state. On the other hand, a decrease in *IS* corresponds to a deterioration in the bonding condition, suggesting a progression toward a fully slip state. When *IS* assumes a value of 0 or ∞, the bonding condition represents one of two extremes: complete slipping or complete bonding, respectively. For intermediate values of *IS*, the bonding condition is classified as a partial-bonding state (Jiang et al., 2021).

3.3. Pavement structure and finite element meshing

The conventional asphalt pavement structure with a flexible base (Huang, 2004) was chosen as the subject of the study. The model, depicted in Figure 4a, consists of three primary layers: the asphalt surface layer AC, the base layer, and the subgrade, and it also shows the material properties for each layer, including thickness *h*, elastic modulus E, and Poisson's ratio μ. In Figure 4b, a key variable in this study is the elastic modulus of the base layer, which was systematically varied. The loading condition simulated a standard dual-wheel single axle with a total load of 100 kN and a tire pressure of 0.7 MPa. The contact area for each tire was modelled with an equivalent radius of 10.65 cm, and the centre-to-centre distance between the dual tires was 31.95 cm. A Cartesian coordinate system was established with its origin at the centre of the dual-wheel gap, where the X, Y, and Z axes represent the driving direction, transverse direction, and depth into the pavement, respectively.

To make the calculations more efficient, a quarter-model with dimensions of 1.0 m (X) × 1.0 m (Y) × 1.25 m (Z) was used, taking advantage of the wheel load's symmetry. The boundary conditions were set as follows: the left (X = 0) and front (Y = 0) planes were defined as symmetric boundaries; the right (X = 1) and bottom (Z = –1.25) boundaries were modelled as infinite elements to simulate a semi-infinite domain; and the top surface was an unconstrained free boundary. The connections between all the pavement layers were modelled as being fully bonded. The mesh had 9716 elements and 45 286 nodes, and most of the elements were 20-node hexagonal ones. To make sure the calculations were correct, a refined, dense mesh was used in the area directly under the wheel load. In areas with a lower stress gradient, the mesh became coarser, as shown in the shaded area of Figure 4c.

a) 1/4 model selection

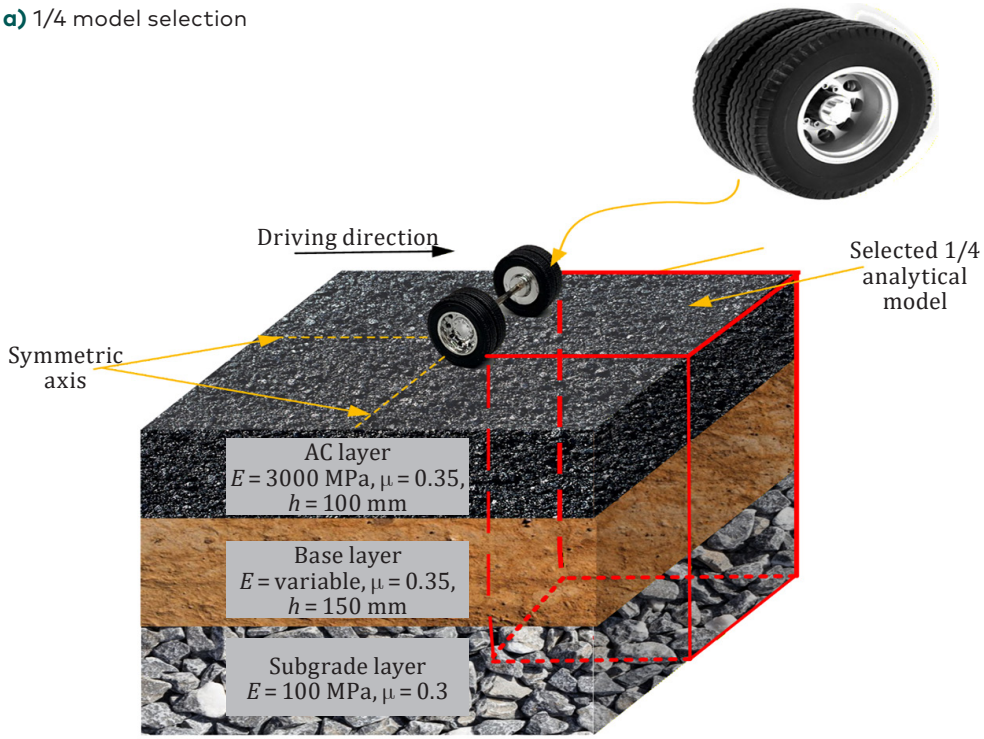

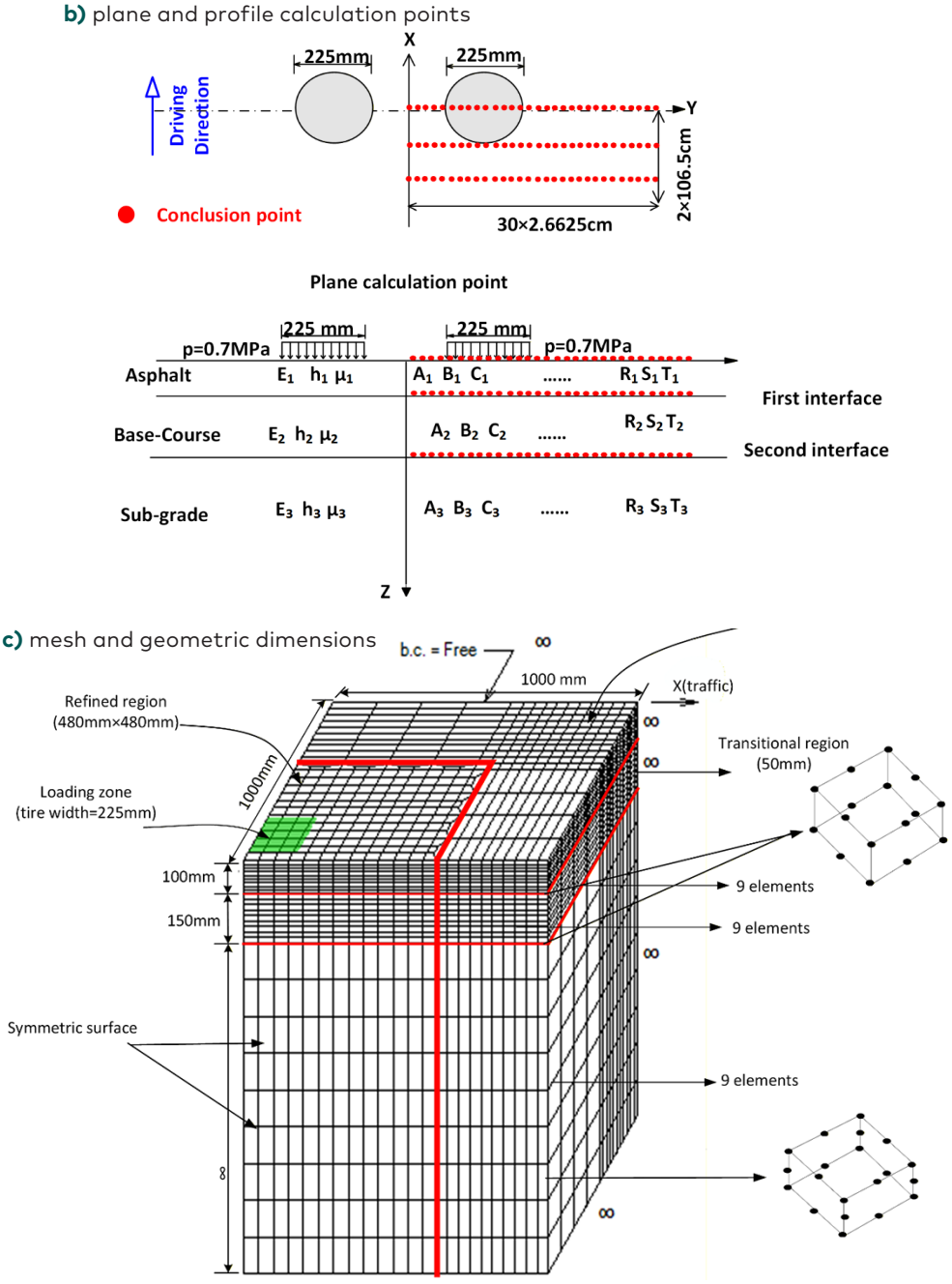

Figure 4. The finite element model

4. Discussion of results

Previously, the maximum critical strains in the asphalt layer consistently occurred beneath the loading zone, as has been noted in many studies (Aarabi & Tabatabaei, 2020; Abu Al-Rub et al., 2012; Al-Hadidy & Tan, 2009; Cortes et al., 2012; Huang et al., 2011; Li et al., 2020; Liu & Shalaby, 2013; Maina et al., 2012; Park & Lytton, 2004). However, the in-plane coordinate of the calculated point utilised in the subsequent analysis in this paper is positioned at the centre of one of the dual tires. It is worth noting that the figures in this section depict one wheel, as the shape is symmetrical in both directions.

4.1. Distribution of deflection at the top of the asphalt layer Uz

Figure 5 examines the deflection of the pavement surface at (x = 0) in the driving direction under different interlayer bonding conditions. Figure 5a depicts the deflection distribution along the asphalt layer for varying R_m values, assuming fully bonded asphalt interfaces. When R_m is low, maximum deflections occur near the wheel centre and the top of the asphalt layer due to weak interlayer bonding. As R_m increases, deflections decrease significantly because stronger bonding reduces deflection, although the rate of improvement slows with further increases in R_m. On the other hand, Figure 5b reveals an irregular concave distribution, identifiable by its distinct curvature, which amplifies deflection at low R_m values, especially near the wheel centre, where load concentration leads to higher deflection.

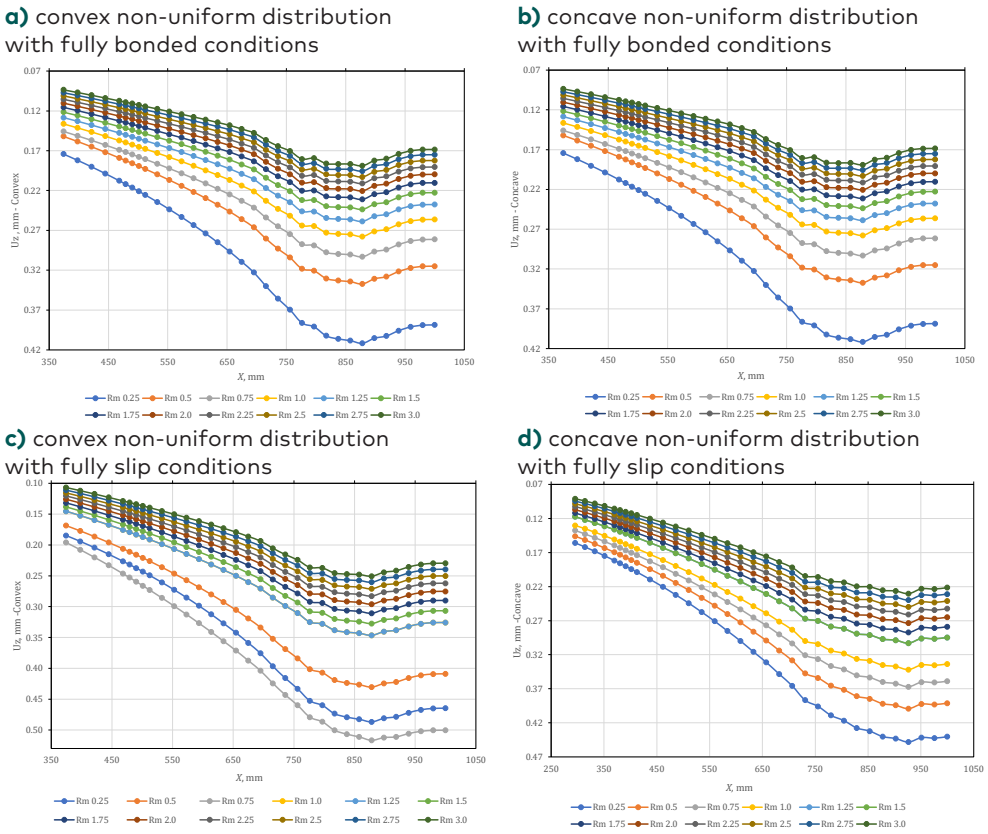

Figure 5. Deflection curves of the pavement under the two extreme interlayer bonding conditions at x = 0 in the driving direction

In the scenario of full slip at first interlayer interfaces, when the load distribution adopts an irregular convex shape, as depicted in Figure 5c, the legend confirms that the highest deflection is observed when the R_m value is 75% of the elastic modulus of the surface layer. This is because greater differential movement at the interfaces occurs under such conditions. The deflection above the surface layer of the pavement begins to decline, as indicated by the data trends in the figure. This reduction may be due to a change in the stress distribution as the load conditions change. In the case of a concave distribution, as illustrated in Figure 5d, the highest deflection occurs at lower R_m values. This phenomenon is because when R_m is low, the interlayer bonding is weaker, allowing for more deflection. As R_m values increase, deflections are reduced because stronger interlayer bonding restricts movement. However, it is indicated that under conditions of complete sliding between the asphalt pavement

surfaces, the pavement becomes increasingly vulnerable to deflection. This is because the lack of proper bonding between the layers allows for greater movement and deflection, potentially leading to the formation of curves on the asphalt surface. This results in the emergence of ripples on the roadway because the uneven deflection causes irregularities in the pavement surface. These ripples adversely affect the smooth movement of vehicles, as they create an uneven driving surface that can cause vibrations and instability.

4.2. Tensile strains at the bottom of asphalt layer ε_{xx}

Figure 6 illustrates the tensile strain along the driving direction at the bottom of the asphalt layer under varying R_m values, different bonding conditions, and diverse loading conditions. This phenomenon indicates that the peak tensile strain in the driving direction is the primary factor inducing fatigue cracking in the asphalt layer. Figure 6a shows a non-uniform convex distribution under full bonding conditions, where the data series with the highest peak in the legend corresponds to an R_m of 0.25. This occurrence is attributed to increased strain concentration resulting from the convex shape, which amplifies the tensile forces at the interface. The plot shows that the peak tensile strains remain stable whenever R_m exceeds 1, signifying that the elastic modulus of the base layer exceeds that of the surface asphalt layer. This stability is facilitated by efficient load distribution that mitigates strain localization at the top layer. Figure 6b presents a non-uniform concave distribution under full bonding conditions, where the curve associated with a lower R_m value-specifically when the elastic modulus of the base layer is significantly less than that of the surface layer-leads to maximum tensile strain. This strain begins to decrease as R_m increases, which can be ascribed to enhanced load transfer efficiency in stiffer materials that reduce strain under applied loads.

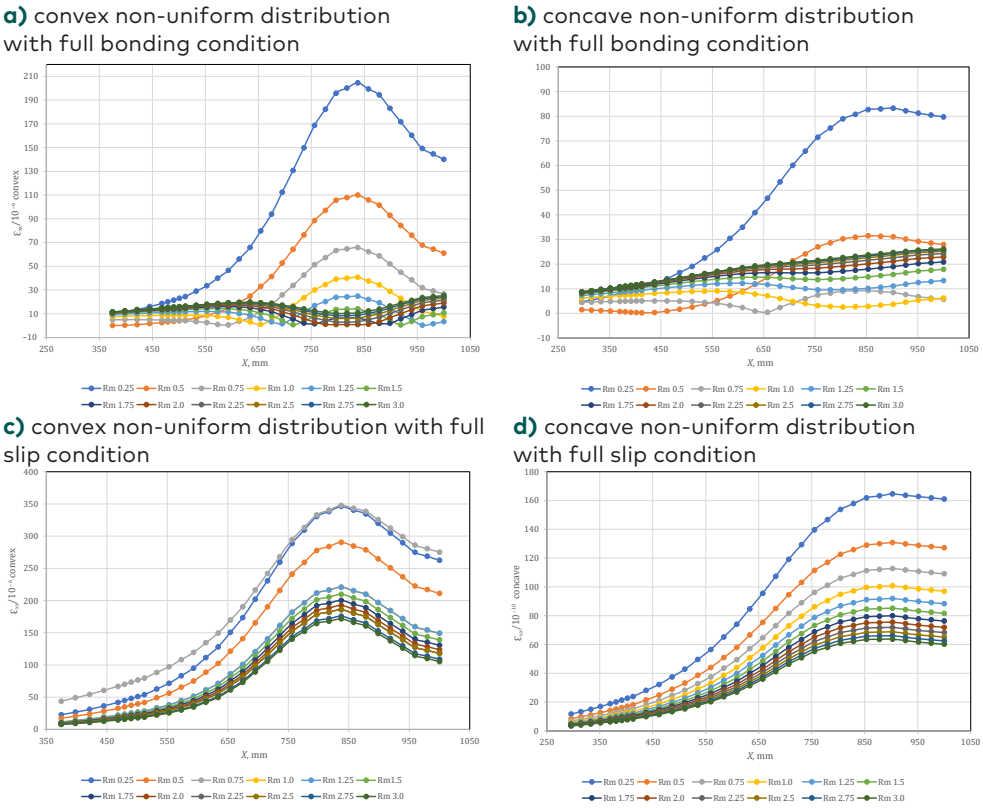

Figure 6. Tensile strains at the bottom of the asphalt layer under the two extreme interlayer bonding conditions at $x = 0$ in the driving direction

In the context of full slip between the interface layers, it is observed that the tensile strain value increases markedly due to the relative motion between the layers that elevates tensile strain, thereby contributing to higher overall strain levels. As shown in Figures 6c and 6d, the tensile strain exhibits a half-sine wave profile, increasing as one approaches the centre of the wheel. The increase in tensile strain is attributed to the relative motion between the layers, which elevates tensile strain. This relationship is supported by the understanding that when two surfaces slide against each other, the frictional forces generated can lead to increased strain in the materials involved. Research has shown that relative motion at the interface can significantly affect the stress distribution, leading to higher strain levels. The half-sine wave profile of the tensile strain is indicative of the load distribution across the pavement. As the load is applied, the strain increases towards the centre of the wheel, reflecting the concentrated load effect. This behaviour is consistent

with findings in pavement mechanics, where tensile strain profiles are often modelled as sinusoidal due to the nature of load application. The sinusoidal shape arises from the way loads are distributed and transferred through the pavement structure. In Figure 6c, a non-uniform convex distribution is depicted under full slip conditions, where the maximum tensile strain is noted by the prominent peak in the profile when R_{m} reaches 0.75. This indicates that the elastic modulus of the base layer is three-quarters that of the surface layer. The increased relative movement enhances the tensile forces experienced at the interface, which is consistent with the principles of material mechanics that state that higher relative motion leads to increased tensile forces. The convex load shape creates areas of concentrated stress, further amplifying the tensile strain. Figure 6d illustrates a non-uniform concave distribution under complete slip between the interface layers of the asphalt pavement structure. The maximum tensile strain occurs whenever R_{m} is low, as highlighted by the corresponding data markers, which is attributed to the significant stiffness disparity that results in excessive strain accumulation under load. Research indicates that when the base layer's stiffness is significantly lower than that of the surface layer, the strain distribution becomes more pronounced, leading to higher tensile strains. The concave shape can exacerbate the effects of load application, resulting in increased strain at the interface.

4.3. Vertical compressive strain of the sub-grade layer ε_{zz}

The vertical compressive strain of the subgrade layer is utilised to forecast its permanent deformation (Maina & Matsui, 2004). Figure 7 demonstrates that the vertical compressive strain in the subgrade layer markedly increases with the elevation of R_{m}, as indicated by the upward trend of all data series in the legend. This indication suggests that a higher modulus of the base layer will result in a decrease in the resistance to permanent deformation of the subgrade layer. This phenomenon is evident across Figures 7a–7d, where the consistent trend confirms the relationship. This happens because a base layer with a high modulus stops the bottom of the subgrade layer from changing shape, while the top of the layer is still affected by the load. This keeps the subgrade layer in a high compressive stress state. Consequently, to effectively control the permanent deformation of the subgrade layer, the modulus of the base layer can be judiciously lowered without causing an increase in the permanent deformation of the subgrade.

a) convex non-uniform distribution with fully bonded condition

b) concave non-uniform distribution under fully bonded conditions

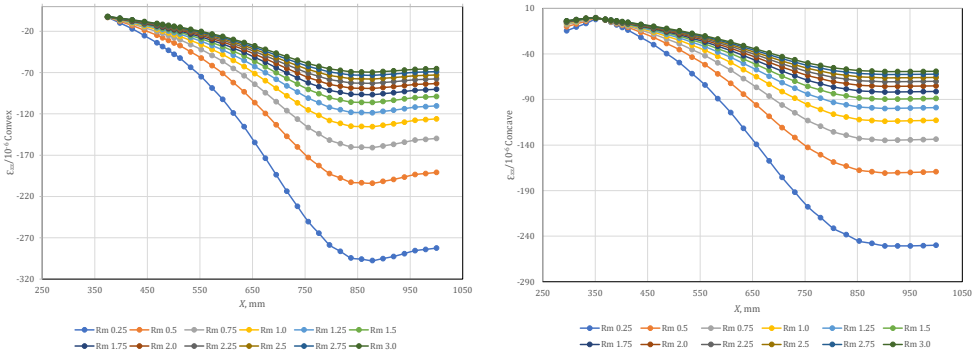

c) convex non-uniform distribution under fully slip conditions

d) concave non-uniform distribution under fully slip conditions

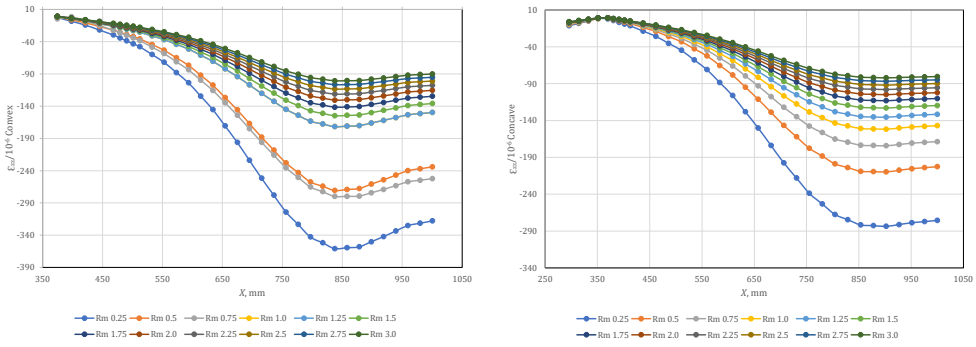

Figure 7. Vertical compressive strain of the sub-grade layer under the two extreme interlayer bonding conditions at $x = 0$ in the driving direction

5. The effect of bonding conditions on the service life of flexible base asphalt pavement

5.1. Transfer function for predicting pavement lifespan

To analyse the influence of bonding conditions on the predicted service life of flexible asphalt pavement under non-uniform wheel loads, this study employed transfer functions (Huang, 2004). These functions, which include fatigue cracking and permanent deformation models as recommended by the American Asphalt Institute (AI) for evaluating pavement structural life, were applied. As described

and illustrated in the subsequent figures, where the service life for different bonding conditions is distinguished by specific markers and line styles in the legend, the service life of a pavement structure under different bonding conditions is estimated.

$$N_{\mathrm{f}} = 0.414\left(\varepsilon\theta\right)^{-3.291}\left|E^{*}\right|^{-0.854} \tag{2}$$

In Equation (2), N_{f} corresponds to the cumulative number of load repetitions contributing to fatigue cracking, $|E^{*}|$ signifies the dynamic modulus of the asphalt mixture expressed in MPa, and εθ represents the horizontal tensile strain at the base of the asphalt layer, which plays a role in fatigue cracking.

$$N_{\mathrm{d}} = 1.365\times10^{-9}\left(\mu_{z}\right)^{-4.477} \tag{3}$$

In Equation (3), N_{d} signifies the total number of load repetitions that influence permanent deformation, while ε_{z} represents the vertical compressive strain that governs this deformation. For a conservative design approach, the highest flexural-tensile strain in the strain in the X direction at the bottom of the asphalt layer was designated as the horizontal tensile strain ε_{θ} to assess fatigue cracking. For permanent deformation, the greatest vertical compressive strain ε_{zz} at the subgrade surface was utilised. To simplify the computational process, the elastic modulus *EE* of the asphalt mixture was employed in Equation (2) as a replacement for its dynamic modulus $|E^{*}|$ (Jiang et al., 2021).

4.4. Effects of the two extreme bonding conditions on the lifespan of the pavement structure

As depicted in Figure 8, the bonding conditions significantly influenced the service life of flexible base asphalt pavement under non-uniform wheel loads. The legend in Figure 8 differentiates the transition from fully bonded to fully slip bonding conditions, which led to a notable decline in N_{f}, the total load repetitions related to fatigue cracking, and N_{d}, the total load repetitions associated with permanent deformation. Both parameters decreased by up to two orders of magnitude, as the logarithmic scale of the plot shows, demonstrating that the deterioration of bonding conditions drastically shortened the pavement's lifespan. However, under these two bonding conditions, the projected structural life of the flexible base asphalt pavement was primarily governed by permanent deformation, as indicated by the lower N_{d} values across all conditions, implying that rutting was the dominant form of pavement damage. A significant disparity in structural life was observed, particularly in practical design and management scenarios. Therefore, steps should be taken to mitigate pavement damage resulting from excessively high tire pressure in flexible base asphalt pavement.

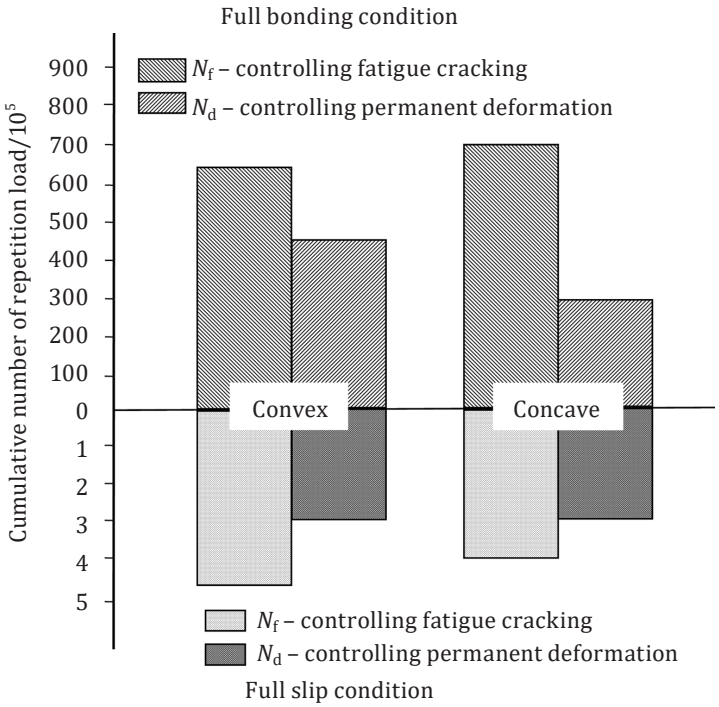

Figure 8. Lifespan of the pavement structure under the two extreme bonding conditions

In summary, this part provides a definitive answer to the question of how bonding conditions affect the service life of flexible base asphalt pavement. The analysis unequivocally demonstrates that the interface condition is a paramount factor, exerting an influence so profound that it can override other design considerations. The transition from a fully bonded to a fully slipped condition was found to catastrophically reduce pavement life, decreasing the allowable load repetitions for both fatigue cracking N_f and permanent deformation N_d by up to two orders of magnitude. This establishes that poor bonding is a primary failure mechanism, drastically accelerating pavement deterioration. Furthermore, the life prediction models confirm that under all bonding scenarios investigated, the structural life is predominantly governed by permanent deformation (rutting) in the subgrade, identifying it as the critical failure mode. Therefore, the central conclusion of this section is that ensuring and maintaining excellent interfacial bonding is not merely beneficial but is a fundamental prerequisite for achieving design life. For pavement engineers, this translates to a critical design imperative: specifying construction techniques and materials that guarantee a fully bonded

system is essential to prevent premature failure and realise the intended long-term performance of flexible pavements.

5. Conclusions and recommendations

5.1. Conclusions

This study employed a 3D finite element model to conduct a parametric analysis of a three-layer flexible pavement system, investigating the effects of base layer modulus R_m, interfacial bonding conditions (full bond vs. full slip), and non-uniform wheel load distributions (convex vs. concave). The following conclusions are drawn from the numerical results:

1. Interfacial bonding is the paramount factor governing service life. The condition at the layer interface exerts a more significant influence on pavement longevity than the stiffness of the base layer. The degradation from a fully bonded to a fully slipped interface resulted in a reduction of the allowable load repetitions (N_f and N_d) by up to two orders of magnitude, representing a life reduction of over 60% for fatigue and 45% for rutting in critical cases. This establishes that superior interfacial bonding is a fundamental requirement to achieve design life.
2. Critical strains are dictated by the load distribution and bonding. The most severe mechanical responses occurred under the effect of a convex load distribution and a fully slipped interface. Specifically:
   – Tensile strain ε_{xx} at the bottom of the asphalt layer reached 348×10^{-6} under full slip with a convex load, which is 70% higher than the 205×10^{-6} recorded under a fully bonded condition with the same load. This drastic increase directly accelerates bottom-up fatigue cracking.
   – Compressive strain ε_{zz} at the top of the subgrade peaked at 365 for the full slip/convex case, compared to 300×10^{-6} for the fully bonded case, indicating a significantly heightened risk of permanent deformation.
3. The dominant failure mode is governed by global system response. For the specific pavement structure analysed, the predicted service life was consistently limited by permanent deformation (rutting) in the subgrade, not fatigue cracking in the asphalt layer, across all scenarios. This finding highlights the importance of evaluating the entire pavement system rather than focusing on a single layer.
4. The efficacy of base layer stiffness is contingent on bonding. The benefit of a high-modulus base layer (high R_m) is fully realised only under perfectly bonded conditions. Under full slip, the structural contribution of a stiff base layer is largely negated, as load transfer is compromised. This indicates that investing in high-quality interface construction is a prerequisite for leveraging the performance benefits of high-performance base materials.

5.2. Recommendations

Based on the findings of this study, the following recommendations are provided.

1. Pavement design guidelines should explicitly incorporate the quality of interfacial bonding as a key design variable. Structural calculations should include sensitivity analyses for imperfect bonding conditions, especially for long-life pavements.
2. The use of optimised tack coats should be mandatory. Construction specifications should include verifiable metrics for interface shear strength, validated through field testing (e.g., Leutner shear test or Torque Bond Test) on cores, to ensure the realisation of a fully bonded system.
3. For the design of highways and major arterials, the critical convex load distribution should be adopted to simulate the high-pressure zones under modern truck tires, as it was proven to generate the most detrimental structural responses.
4. The selection of the base layer material should be based on a systems approach that prioritises bendability and stiffness compatibility with the asphalt layer, rather than maximising base stiffness alone.
5. The parametric nature of this study necessitates future validation to enhance its predictive credibility. Subsequent research should focus on:
   - conducting full-scale or large-scale laboratory experiments with instrumented pavement sections to measure strain responses under controlled loading and predefined bonding conditions for direct model calibration;
   - instrumenting in-service pavement sections to monitor long-term performance under real traffic, providing data to correlate the modelled strain responses with actual observed distress;
   - developing and validating models for partial bond conditions, which represent the most common real-world scenario, to create a more granular understanding of interface performance.

Conflict of interest

The authors declare that they have no conflict of interest.

Statement of the use of generative AI and AI-assisted technologies in the writing process

This manuscript was written by the authors and did not rely on artificial intelligence for its creation.

REFERENCES

Aarabi, S., & Tabatabaei, S. A. (2020). Viscoelastic analysis of thickness variation of asphaltic pavements under repeated loading using finite element method. *International Journal of Pavement Engineering*, *21*(2), 203–214. https://doi.org/10.1080/10298436.2018.1450504

Abed, A., Thom, N., & Neves, L. (2019). Probabilistic prediction of asphalt pavement performance. *Road Materials and Pavement Design*, *20*(S1), S247–S264. https://doi.org/10.1080/14680629.2019.1593229

Abu Al-Rub, R. K., Darabi, M. K., Huang, C. W., Masad, E. A., & Little, D. N. (2012). Comparing finite element and constitutive modelling techniques for predicting rutting of asphalt pavements. *International Journal of Pavement Engineering*, *13*(4), 322–338. https://doi.org/10.1080/10298436.2011.566613

Al-Hadidy, A. I., & Tan, Y. Q. (2009). Mechanistic analysis of ST and SBS-modified flexible pavements. *Construction and Building Materials*, *23*(8), 2941–2950. https://doi.org/10.1016/j.conbuildmat.2009.02.023

Anghelache, G., & Moisescu, R. (2012). Measurement of stress distributions in truck tyre contact patch in real rolling conditions. *Vehicle System Dynamics*, *50*(12), 1747–1760. https://doi.org/10.1080/00423114.2012.674143

Arshad, M. (2018). Correlation between resilient modulus (*MR*) and constrained modulus (*MC*) values of granular materials. *Construction and Building Materials*, *159*, 440–450. https://doi.org/10.1016/j.conbuildmat.2017.10.047

Arulrajah, A., Disfani, M. M., Haghighi, H., Mohammadinia, A., & Horpibulsuk, S. (2015). Modulus of rupture evaluation of cement stabilized recycled glass/recycled concrete aggregate blends. *Construction and Building Materials*, *84*, 146–155. https://doi.org/10.1016/j.conbuildmat.2015.03.048

Assogba, O. C., Tan, Y., Zhou, X., Zhang, C., & Anato, J. N. (2020). Numerical investigation of the mechanical response of semi-rigid base asphalt pavement under traffic load and nonlinear temperature gradient effect. *Construction and Building Materials*, *235*, Article 117406. https://doi.org/10.1016/j.conbuildmat.2019.117406

Bassim, R., & Issa, M. (2020). Dynamic- and static-elastic moduli and strength properties of early-age Portland cement concrete pavement mixtures. *Journal of Materials in Civil Engineering*, *32*(5), Article 3089. https://doi.org/10.1061/(ASCE)MT.1943-5533.0003089

Bestgen, J. O., Hatipoglu, M., Cetin, B., & Aydilek, A. H. (2016). Mechanical and environmental suitability of recycled concrete aggregate as a highway base material. *Journal of Materials in Civil Engineering*, *28*(9), Article 1564. https://doi.org/10.1061/(ASCE)MT.1943-5533.0001564

Bhandari, S., Luo, X., & Wang, F. (2023). Understanding the effects of structural factors and traffic loading on flexible pavement performance. *International Journal of Transportation Science and Technology*, *12*(1), 258–272. https://doi.org/10.1016/j.ijtst.2022.02.004

Bilodeau, J. P., & Doré, G. (2012). Relating resilient behaviour of compacted unbound base granular materials to matrix and interlock characteristics. *Construction and Building Materials*, *37*, 220–228. https://doi.org/10.1016/j.conbuildmat.2012.07.036

Canestrari, F., & Ingrassia, L. P. (2020). A review of top-down cracking in asphalt pavements: Causes, models, experimental tools, and future challenges. *Journal of Traffic and Transportation Engineering (English Edition)*, *7*(5), 541–572. https://doi.org/10.1016/j.jtte.2020.08.002

Cetin, B., Aydilek, A. H., & Guney, Y. (2010). Stabilization of recycled base materials with high carbon fly ash. *Resources, Conservation and Recycling*, *54*(11), 878–892. https://doi.org/10.1016/j.resconrec.2010.01.007

Chen, C. (2017). Science mapping: A systematic review of the literature. *Journal of Data and Information Science*, *2*(2), 1–40. https://www.researchgate.net/publication/313991204_Science_Mapping_A_Systematic_Review_of_the_Literature

Cortes, D. D., Kim, H. K., & Palomino, A. M. (2012). Simulation of inverted pavement systems. *Geotechnical and Geological Engineering*, *30*(2), 291–305.

da Conceição Leite, F., dos Santos Motta, R., Vasconcelos, K. L., & Bernucci, L. (2011). Laboratory evaluation of recycled construction and demolition waste for pavements. *Construction and Building Materials*, *25*(6), 2972–2979. https://doi.org/10.1016/j.conbuildmat.2010.11.105

Dhasmana, H. (2020). *Mechanistic characterization of thin asphalt overlays for pavement preservation*. University of Illinois at Urbana-Champaign.

El-Kholy, S. A., & Galal, S. A. (2012). A study on the effects of non-uniform tyre inflation pressure distribution on rigid pavement responses. *International Journal of Pavement Engineering*, *13*(3), 244–258. https://doi.org/10.1080/10298436.2011.623780

Fan, J., & Njuguna, J. (2016). An introduction to lightweight composite materials and their use in transport structures. In *Lightweight Composite Structures in Transport* (pp. 3–34). Woodhead Publishing. https://doi.org/10.1016/B978-1-78242-325-6.00001-3

Gu, H., Jiang, X., Li, Z., Yao, K., & Qiu, Y. (2019). Comparisons of two typical specialized finite element programs for mechanical analysis of cement concrete pavement. *Mathematical Problems in Engineering*, *2019*, Article 9178626. https://doi.org/10.1155/2019/9178626

Haider, S. W., Chatti, K., Buch, N., Lyles, R. W., Pulipaka, A. S., & Gilliland, D. (2007). Effect of design and site factors on the long-term performance of flexible pavements. *Journal of Performance of Constructed Facilities*, *21*(4), 283–292. https://doi.org/10.1061/(ASCE)0887-3828(2007)21:4(283)

Harri, J., Filali, F., & Bonnet, C. (2009). Mobility models for vehicular ad hoc networks: A survey and taxonomy. *IEEE Communications Surveys & Tutorials*, *11*(4), 19–41. https://doi.org/10.1109/SURV.2009.090403

Hernandez, J. A., & Al-Qadi, I. L. (2016a). Contact phenomenon of free-rolling wide-base tires: Effect of speed and temperature. *Journal of Transportation Engineering*, *142*(12), Article 893. https://doi.org/10.1061/(ASCE)TE.1943-5436.0000893

Hernandez, J. A., & Al-Qadi, I. L. (2016b). Hyperelastic modeling of wide-base tire and prediction of its contact stresses. *Journal of Engineering Mechanics*, *142*(2), Article 1007. https://doi.org/10.1061/(ASCE)EM.1943-7889.0001007

Hernandez, J. A., & Al-Qadi, I. L. (2017). Semicoupled modeling of interaction between deformable tires and pavements. *Journal of Transportation Engineering, Part A: Systems*, *143*(4), Article 7. https://doi.org/10.1061/JTEPBS.0000007

Hu, X. D., & Sun, J. (2005). Measuring tire ground pressure distribution of heavy vehicle. *Tongji Daxue Xuebao/Journal of Tongji University (Natural Science)*, *33*(11), 1443–1448.

Hu, X. D., & Sun, L. (2006). Stress response analysis of asphalt pavement under measured tire ground pressure of heavy vehicle. *Journal-Tongji University*, *34*(1), Article 64.

Huang, C. W., Abu Al-Rub, R. K., Masad, E. A., & Little, D. N. (2011). Three-dimensional simulations of asphalt pavement permanent deformation using a nonlinear viscoelastic and viscoplastic model. *Journal of Materials in Civil Engineering*, *23*(1), 56–68. https://doi.org/10.1061/(ASCE)MT.1943-5533.0000022

Huang, Y. H. (2004). *Pavement analysis and design* (2nd ed.). Pearson.

Ijari, K., & Paternina-Arboleda, C. D. (2024). Sustainable pavement management: Harnessing advanced machine learning for enhanced road maintenance. *Applied Sciences*, *14*(15), Article 6640. https://doi.org/10.3390/app14156640

Ilse, M. (2015). Evaluation of tire/surfacing/base contact stresses and texture depth. *International Journal of Transportation Science and Technology*, *4*(1), 107–118. https://doi.org/10.1260/2046-0430.4.1.107

Ji, X., Hou, Y., Li, X., & Wang, T. (2019). Comparison on properties of cement-stabilised gravel prepared by different laboratory compaction methods. *Road Materials and Pavement Design*, *20*(4), 991–1003. https://doi.org/10.1080/14680629.2017.1423105

Jiang, B., Xu, L., Cao, Z., Yang, Y., Sun, Z., & Xiao, F. (2024). Interlayer distress characteristics and evaluations of semi-rigid base asphalt pavements: A review. *Construction and Building Materials*, *431*, Article 136441. https://doi.org/10.1016/j.conbuildmat.2024.136441

Jiang, X., Zeng, C., Yao, K., Gu, H. Y., Li, Z. K., & Qiu, Y. J. (2021). Influence of bonding conditions on flexible base asphalt pavement under non-uniform vertical loads. *International Journal of Pavement Engineering*, *22*(12), 1491–1503. https://doi.org/10.1080/10298436.2019.1697441

Jiang, Y. J., & Fan, L. F. (2013). An investigation of mechanical behavior of cement-stabilized crushed rock material using different compaction methods. *Construction and Building Materials*, *48*, 508–515. https://doi.org/10.1016/j.conbuildmat.2013.07.017

Leon, L., & Charles, R. (2015). Impact of coarse aggregate type and angularity on permanent deformation of asphalt concrete. *WIT Transactions on Modelling and Simulation*, *59*, 303–313. https://doi.org/10.2495/CMEM150271

Leon, L., Gay, D., Simpson, N., & Edwin, S. (2019). Stress-strain and failure modes of asphalt concrete in compression due to geometrical changes. *5th International Conference on Road and Rail Infrastructure*, Zadar, Croatia. https://doi.org/10.5592/CO/CETRA.2018.846

Leon, L. P., & Gay, D. (2020). Finite element modelling of repeated load axial test of laboratory cylindrical HMA using constitutive creep model. *International Conference on Transportation and Development 2020*, 41–50. https://doi.org/10.1061/9780784483183.005

Leon, L. P., & Ray, I. (2021). Estimating unconfined compressive behavior of HMA using soft computing. *Innovative Infrastructure Solutions*, *6*(1), Article 19. https://doi.org/10.1007/s41062-020-00386-9

Li, J., White, D. J., Stephenson, W. R., & Li, C. (2019). Considerations for laboratory resilient modulus testing of unbound pavement base materials. *Construction and Building Materials*, *195*, 515–523. https://doi.org/10.1016/j.conbuildmat.2018.11.049

Li, J., Zhang, X., & Wang, L. (2020). Comparison of BISAR3.0 and EverStressFE for interlayer bonding analysis. *Road Materials and Pavement Design*, *21*(6), 1567–1582.

Liu, Q., & Shalaby, A. (2013). Simulation of pavement response to tire pressure and shape of contact area. *Canadian Journal of Civil Engineering*, *40*(3), 236–242. https://doi.org/10.1139/cjce-2011-0567

Maina, J. W., & Matsui, K. (2004). Developing software for elastic analysis of pavement structure responses to vertical and horizontal surface loadings. *Transportation Research Record*, *1896*(1), 107–118. https://doi.org/10.3141/1896-11

Maina, J. W., Ozawa, Y., & Matsui, K. (2012). Linear elastic analysis of pavement structure under non-circular loading. *Road Materials and Pavement Design*, *13*(3), 403–421. https://doi.org/10.1080/14680629.2012.705419

Miao, Y., Huang, Y., Zhang, Q., & Wang, L. (2016). Effect of temperature on resilient modulus and shear strength of unbound granular materials containing fine RAP. *Construction and Building Materials*, *124*, 1132–1141. https://doi.org/10.1016/j.conbuildmat.2016.08.137

Mohammad, L. N., Raghavandra, A., & Huang, B. (2000). Laboratory performance evaluation of cement-stabilized soil base mixtures. *Transportation Research Record*, *1721*(1), 19–28. https://doi.org/10.3141/1721-03

Norouzi, A., Kim, D., & Richard Kim, Y. (2016). Numerical evaluation of pavement design parameters for the fatigue cracking and rutting performance of asphalt pavements. *Materials and Structures*, *49*, 3619–3634. https://doi.org/10.1617/s11527-015-0744-x

Nouri, A., Shirvan, A. R., Li, Y., & Wen, C. (2021). Additive manufacturing of metallic and polymeric load-bearing biomaterials using laser powder bed fusion: A review. *Journal of Materials Science & Technology*, *94*, 196–215. https://doi.org/10.1016/j.jmst.2021.03.058

Oliver, W. C., & Pharr, G. M. (2004). Measurement of hardness and elastic modulus by instrumented indentation: Advances in understanding and refinements to methodology. *Journal of Materials Research*, *19*(1), 3–20. https://doi.org/10.1557/jmr.2004.19.1.3

Park, S. W., & Lytton, R. L. (2004). Effect of stress-dependent modulus and Poisson's ratio on structural responses in thin asphalt pavements. *Journal of Transportation Engineering*, *130*(3), 387–394. https://doi.org/10.1061/(ASCE)0733-947X(2004)130:3(387)

Poon, L. P. (2020). Aggregates angularity effects on mechanical properties of asphalt concrete. *The International Conference on Emerging Trends in Engineering and Technology (IConETech-2020)*. https://doi.org/10.47412/WCLJ3100

Qian, Z., Liu, Y., & Zheng, Y. (2021). Discrepancies between theoretical and measured pavement responses: A systematic error analysis. *International Journal of Pavement Engineering*, *22*(14), 1783–1795.

Romeo, E., Orazi, M., Orazi, U. S., Accardo, C., Noto, S., & Tebaldi, G. (2019). Evaluation of "long-term behaviour under traffic" of cement treated mixture with RAP. *Construction and Building Materials*, *208*, 421–426. https://doi.org/10.1016/j.conbuildmat.2019.03.045

Selsal, Z., Karakas, A. S., & Sayin, B. (2022). Effect of pavement thickness on stress distribution in asphalt pavements under traffic loads. *Case Studies in Construction Materials*, *16*, Article e01107. https://doi.org/10.1016/j.cscm.2022.e01107

Singh, A. K., & Sahoo, J. P. (2021). Rutting prediction models for flexible pavement structures: A review of historical and recent developments. *Journal of Traffic and Transportation Engineering (English Edition)*, *8*(3), 315–338. https://doi.org/10.1016/j.jtte.2021.04.003

Sofwan, A., Soetrisno, Y. A. A., Ramadhani, N. P., Rahmayani, A., Handoyo, E., & Arfan, M. (2019). Vehicle distance measurement tuning using Haversine and micro-segmentation.

2019 International Seminar on Intelligent Technology and Its Applications (ISITIA), Surabaya, Indonesia, 239–243. https://doi.org/10.1109/ISITIA.2019.8937128

Solanki, P., Khoury, N., & Zaman, M. M. (2009). Engineering properties and moisture susceptibility of silty clay stabilized with lime, class C fly ash, and cement kiln dust. *Journal of Materials in Civil Engineering*, *21*(12), 749–757. https://doi.org/10.1061/(ASCE)0899-1561(2009)21:12(749)

Szczucka-Lasota, B., Węgrzyn, T., Łazarz, B., & Kamińska, J. A. (2021). Tire pressure remote monitoring system reducing the rubber waste. *Transportation Research Part D: Transport and Environment*, *98*, Article 102987. https://doi.org/10.1016/j.trd.2021.102987

Titus-Glover, L., Darter, M. I., & Von Quintus, H. L. (2019). *Impact of environmental factors on pavement performance in the absence of heavy loads* (Report No. FHWA-HRT-16-084). United States. Federal Highway Administration. https://www.fhwa.dot.gov/publications/research/infrastructure/pavements/16084/16084.pdf

Wang, F. (2005). *Mechanistic-empirical study of effects of truck tire pressure on asphalt pavement performance* [Doctoral dissertation, The University of Texas at Austin]. https://repositories.lib.utexas.edu/server/api/core/bitstreams/e1241496-2810-42a2-ad7b-85b6a4180d2a/content

Wang, H. (2011). *Analysis of tire-pavement interaction and pavement responses using a decoupled modeling approach* [Doctoral dissertation, University of Illinois at Urbana-Champaign]. https://www.ideals.illinois.edu/items/25037

Wang, H., Al-Qadi, I. L., & Stanciulescu, I. (2012). Simulation of tyre-pavement interaction for predicting contact stresses at static and various rolling conditions. *International Journal of Pavement Engineering*, *13*(4), 310–321. https://doi.org/10.1080/10298436.2011.565767

Wei, S., Wang, Y., Cheng, H., & Wang, D. (2021). Stress distributions in the textures of prefabricated pavement surface created with the assistance of 3D printing technology. *International Journal of Pavement Engineering*, *24*(1), 1–17. https://doi.org/10.1080/10298436.2021.2005058

Yao, K., Jiang, X., Jiang, J., Yang, Z., & Qiu, Y. (2021). Influence of modulus of base layer on the strain distribution for asphalt pavement. *The Baltic Journal of Road and Bridge Engineering*, *16*(4), 126–152. https://doi.org/10.7250/bjrbe.2021-16.542

Zaumanis, M., Mallick, R. B., & Frank, R. (2014). 100% recycled hot mix asphalt: A review and analysis. *Resources, Conservation and Recycling*, *92*, 230–245. https://doi.org/10.1016/j.resconrec.2014.07.007

Zhu, H., & Shi, L. (2021). Application of typical engineering. In *Methodology of Highway Engineering Structural Design and Construction. Advanced Topics in Science and Technology in China,* vol. 59 (pp. 73–231). Springer, Singapore. https://doi.org/10.1007/978-981-15-6544-1_5